Proceedings World Geothermal Congress 2005
Antalya, Turkey, 24-29 April 2005

Petrophysical Parameters of Rocks Saturated with Liquid Water at High Temperature Geothermal Reservoir Conditions

J. Kulenkampff 1), E. Spangenberg 1), O. Flovenz 2), S. Raab 1) and E. Huenges 1)

1) GeoForschungsZentrum Potsdam (GFZ), Telegrafenberg, 14473 Potsdam, Germany

2) Iceland GeoSurvey (ÍSOR), Grensásvegi 9, 108 Reykjavík, Iceland

Keywords: High temperature petrophysics, geophysics, reservoir engineering

ABSTRACT

A laboratory system for the investigation of water saturated rocks at temperatures up to 250 °C and controlled confining and pore pressures up to 50 MPa was developed and successfully applied for investigations on rock samples from Icelandic high temperature geothermal fields. The samples were selected from a core-collection of deep boreholes at Iceland GeoSurvey.

The samples came from depths where the ambient temperature is in the range 150-230°C and both from the smectite and the chlorite alteration zones.

Four-electrode resistivity, compressional and shear wave velocity were measured at equilibrated temperatures ranging from 25°C to 230°C and at estimated in-situ pore and confining pressure. The samples were exposed to these conditions for periods up to some days to investigate their stability.

Three out of six samples were successfully measured over 200°C. Two of them are from the chlorite alteration zone and one from the smectite zone. All the three samples show much stronger temperature dependence of the conductivity than expected from pore fluid conduction. This indicates that surface conduction is the dominant conduction mechanism. The temperature dependence of the compressional wave velocity above 100°C is similar to what could be expected from the temperature dependence of the velocity in pure water.

1. INTRODUCTION

Geophysical field and borehole measurements are used for the rough evaluation of high temperature (H.T.) geothermal reservoirs. Exploration methods make use of a typical resistivity structure of H.T. reservoirs that is related to the isotherms. It shows a hot core of high resistivity with temperatures above 200°C underlying a zone with low resistivity and lower temperatures, down to 70°C (Árnason and Flóvenz, 1992, Ussher et al. 2000). This low resistive zone with resistivities generally lower than 5 Ωm coincides with the smectite-zeolite alteration zone, while the resistivity increase towards the hotter central zone is related to the transition to the mixed layer clay and the chlorite/epidot alteration zone (Arnasson et al. 2000). On the basis to the evolution of the specific internal surface area and surface bound charge distributions, the predominant conduction mechanism has been postulated to change from electrolytic free pore fluid conduction in the unaltered surface zone to interface conduction in the smectite-zeolite zone, and back to volume conduction in the central zone (Árnason and Flóvenz, 1992, Flóvenz et al. 1985).

These fluid-solid interactions can considerably change the physical rock properties. Interlayer conduction processes, which are due to the existence of excess charges in the electrical double layer, can explain the occurrence of characteristic resistivity structures found in geothermal fields.

However, little specific is known about petrophysical parameters at reservoir conditions from controlled laboratory experiments. These conditions are often characterized by temperatures exceeding 200 °C and pore pressures of around 10 MPa, with the pore water being in the liquid phase, posing experimental difficulties comparable to well-logging in 200°C hot wells.

The physical properties of the salt solutions in the pores and the dry minerals are fairly known up to 200°C, but near the critical point (for clean water: 374°C and 22 MPa) both the experimental data base and the theory of electrolytic solutions becomes weak.

There exist very little data of water-saturated rocks with controlled pore pressure at high-temperature conditions. Interactions between the solids and the liquid water probably become more essential above 100°C than at ambient conditions, because clay minerals are altered above this temperature range. Llera et al (1990) measured resistivity of mainly dacite tuffs in the range up to 250°C, but as short term heating experiments without due time for stabilization. Duba et al (1997) tried to attain more stable conditions up to 150°C, but could not apply high enough pressure to prevent the water from boiling.

The purpose of this study was to investigate the temperature behavior of volcanic rocks from different alteration zones of Icelandic geothermal reservoirs, containing low saline liquid water. The samples were saturated by in-situ like pore fluid and exposed to temperatures up to 250 °C at the assumed in-situ pore and confining pressures for periods long enough for temperature equilibration and for short term alteration processes which could change surface properties of the mineral grains.

2. TEMPERATURE EFFECTS ON RESISTIVITY AND ULTRASONIC VELOCITY

2.1 Fluid Effects

On first impression thermophysical properties of water and steam appear to be well known and completely understood. This is approximately true in the vicinity of ambient conditions, but at higher pressures and temperatures data are becoming scarce, and “dense water” at these conditions is still subject of recent physico-chemical research (Franck and Weingärtner 1999).

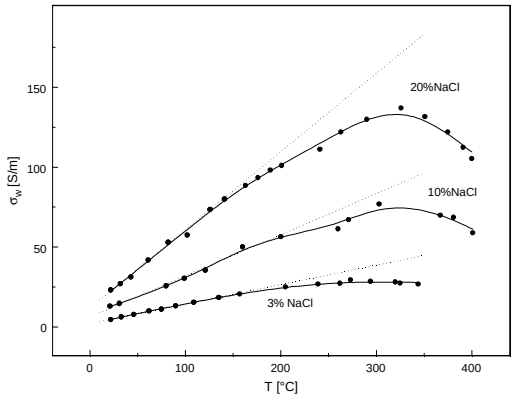

Figure 1: Electrical conductivity of 3%-, 10%-, and 20%-NaCl-solutions. Data from Ucok *et al.* (1980).

Temperature and pressure effects are usually described by linear coefficients around ambient pressure and temperature conditions; however, approaching the critical point the deviations from the linear behavior become significant. Ho *et al.* (1994) reported a linear increase of equivalent conductance of NaCl solutions below 300°C, reaching constant values at higher temperature. The conductivity of the solutions is therefore controlled by the decrease of fluid density with increasing temperature. Ucok *et al.* (1980) measured electrical resistivities of representative geothermal brines up to the critical point. Conductivities calculated from their results are linearly increasing with temperature below 150°C and generally decreasing above 250°C (Fig. 1). This effect is caused by the temperature dependences of density, viscosity, and dielectric permittivity. These data are available at the NIST Chemistry WebBook (Lemmon et al. 2003).

Below 150°C the increase in fluid conductivity is described by linear temperature dependence, according to

$$\sigma_w(T) = \sigma_w(T_0) \cdot (1 + \alpha_f (T - T_0)) \qquad (1)$$

where σ_w is the water conductivity and α_f the temperature coefficient. Revil *et al.* (1998), like the well-known Arps formula (Arps 1953) which is used as a basis for Log Interpretation Charts, assume a temperature coefficient of 0.02/° at 20°C.

The sound speed in water is available at the NIST Chemistry Webbook (Lemmon *et al.* 2003) as well. Its strong decrease with increasing temperature is due to the decreasing compressibility that overcompensates the density decrease (Fig. 2).

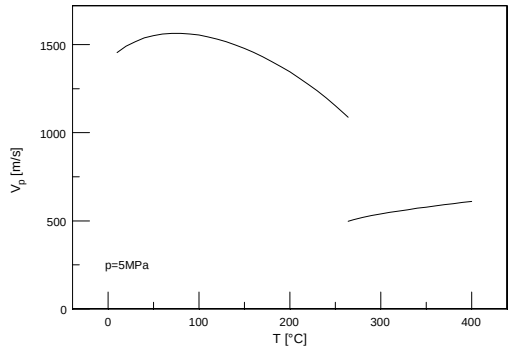

Figure 2: Sound speed in pure water at 5 MPa. The discontinuity at 264 °C is due to the boiling point. Data from the NIST Chemistry Webbook (Lemmon *et al.* 2003).

Another issue is the strong pressure and temperature dependence of the static dielectric permittivity, which plays a major role for the strength of electrostatic interactions and thus for both solution processes and rock-fluid interactions (Fernandez et al. 1997).

2.2 Resistivity Effect of Rock-Water Interactions

The electrical conductivity of fluid saturated rocks is a combined effect of the free fluid that is distributed in the pore space, and the interlayer conductivity of space charges at the grain boundaries (electric double layer). In a first approximation free fluid and interlayer conductivity are acting in parallel. The free fluid conductivity is controlled by the formation factor F, and the interlayer conductivity depends on the surface charge density, i.e. the specific internal surface area, fluid and grain compositions, and an interlayer conductance term:

$$\sigma_0(T, p, c) = \frac{\sigma_w(T, p, c)}{F} + G_\delta(T, p, c) \cdot S_{por} \qquad (2)$$

where σ_0, σ_w, F, S_{por}, G_δ are rock and water conductivity, formation factor, pore volume specific internal surface area and interlayer conductance, respectively (Rink and Schopper, 1974). These parameters depend on temperature T, pressure p and electrolyte concentration c. A possible T-p-c-dependence of S_{por} and F, which considers alteration and pressure effects on the pore structure, is neglected.

The surface conductance is a complicated function of the thermodynamic variables. It depends on the distribution of space charges in the interlayer and their mobility:

$$G_\delta(T, p, c) = \int_0^{R(T,p,c)} \mu(T, p, c_s(r)) \cdot c_s(r)\, dr \qquad (3)$$

where μ is the mobility of excess charges in the interlayer and $c_s(r)$ their distribution. R is the thickness of the interlayer, which is affected by excess charges. The charge distribution, which is controlled by the Poisson-Boltzmann equation, incorporates explicit and implicit temperature terms (i.e. surface charge density, dielectric permittivity, ionic strength) (Reppert and Morgan 2003).

Below 200 °C a linear approximation with a temperature coefficient of 0.04/°C reasonably reflects the temperature dependence of interlayer conductivity (Revil *et al.* 1998), in spite of this complicated theory. However, similar deviations as for ionic solutions are expected at higher temperatures.

It should be mentioned that osmotic forces between overlapping electric double layers might contribute to the elastic moduli and the absorption of sound waves in fluid saturated rocks. These effects are described by the DLVO-theory (Israelachvili, 1992), which is based on the same rock-water interaction effects as the electric interlayer conductivity. Thus, similar temperature effects on ultrasonic waves have to be considered.

3. EXPERIMENTALS

3.1 "Field Laboratory Experimental Core Analysis System" (FLECAS)

FLECAS (Fig. 3) was originally designed as a versatile system for the investigation of terrestrial gas hydrate

bearing sediments under in-situ conditions (Kulenkampff and Spangenberg 2004), which means a temperature range between –20°C to 30°C.

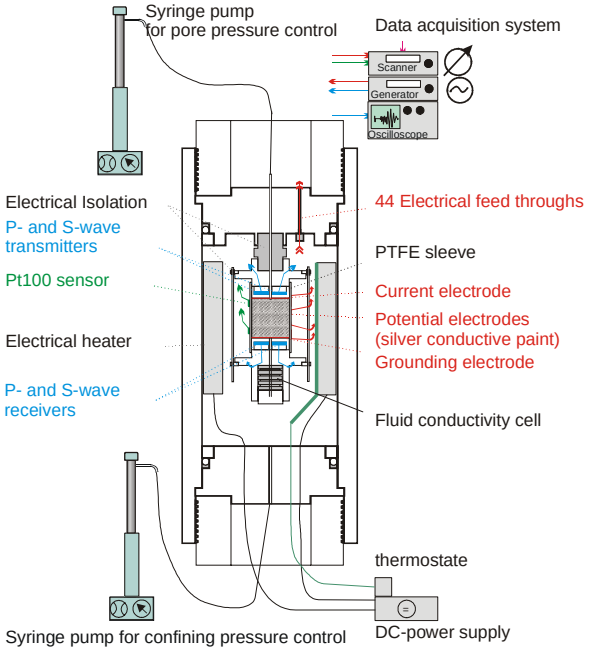

Figure 3: Schematic diagram of the Field Laboratory Experimental Core Analysis System (FLECAS).

The system was equipped with an electrical heating and sealings made of heat-resistant materials (PEEK, FPM, PTFE) in order to withstand temperatures up to 250°C. It comprises syringe pumps for the control of the hydrostatic confining pressure (up to 70 MPa) and the pore fluid pressure (up to 40 MPa), electrodes for four-electrode resistivity measurements, and P-wave and S-wave transducers. The piezo shear and compressional transducers with a resonance frequency of 500 kHz are installed in close contact to the samples in the end caps, which at the same time serve as current electrodes for the resistivity measurements. Ring electrodes around the sample out of silver conductive paint are used as potential electrodes that are contacted through the PTFE-jacket. A voltage of 1 V and 15 Hz is applied to the end caps and generates the current for resistivity monitoring. Both 2-electrode and 4-electrode resistivities are recorded during the whole experiment by simply measuring the current and the voltages. When the equilibrium conditions – constant temperature and resistivity - were reached precise selective frequency dependent electrical impedance measurements in the frequency range from 0.01 Hz to 1 kHz were made with a Zahner IM6 electrochemical workstation (EIS: Electrical Impedance Spectrometry). Both measurements are in fair accordance, although the simple resistivity monitoring is affected by noise.

The detection and picking of the P-waves, transmitted and recorded with P-wave transducers, was a simple and accurate procedure. However, the detection of the S-waves is faulty, probably with cycle-skipping, even though transmitter and receiver were both S-wave transducers.

3.2 Samples

The cores from Icelandic geothermal wells were dry and have been stored at room conditions for several years (Tab. 1). 6 cylindrical samples (length 50 mm, diameter 47.6 mm) were prepared from the cores. They were vacuum dried and then saturated with low saline water solutions that were prepared with Na^+, K^+, Cl^-, SO_4^{2-} according to the main constituents of the formation fluids.

Table 1. Overview of the sample used in the experiments. The K-samples are from the Krafla high temperature field in N-Iceland, K-9 from well no. KG-2 and K51, K52 and K-58 from well no. KH-3. The NJ-samples are from well no. NJ-17 at the Nesjavellir high temperature field in SV-Iceland. T_f is the estimated formation temperature and σ_w the pore water conductivity.

Sample	Depth [m]	Material / Alteration	T_f [°C]	σ_w [S/m]
K9	540	Basalt / Chlorite	ca. 200	0.078
K51	164.7	Basalt / Smectite	ca. 150	0.078
K52	168.2	Basalt / Smectite	ca. 150	0.078
K58	187.5	Basalt / Smectite	ca. 160	0.078
NJ1	1005	Hyaloclastite / Chlorite	230	0.051
NJ6	1005	Hyaloclastite / Chlorite	230	0.051

The formation factors that were determined on similar samples were generally higher than 100, in accordance with low porosities (<10%) (Flóvenz et al., 2005). In combination with the low salinity of the pore water the effect of surface conductivity (Eq. (1)) is accentuated.

3.3 Procedure

The measurement sequence was conducted slowly in order to achieve equilibrated sample temperatures, stepwise ranging from 25°C to 230°C, and at estimated in-situ pore and confining pressure. This equilibration period for each step was at least 5 hours. At some points, the samples were exposed to these conditions for longer periods, up to some days, to investigate possible alteration effects. Both pore and confining pressures were stabilized by the syringe pumps during the whole procedure.

The thermal stability of the feed-through (PEEK) was exceeded above 230 °C, where all experiments terminated after some hours at the latest. Three of the six samples (K1, K9, NJ1) were exposed to 230 °C; otherwise the experiments finished at lower temperatures as a result of other defects.

3.3 The progress of the experiments

The measuring records are shown in Figs. 4 - 11. Temperature dependent P-waves and 2-electrode resistivity were recorded for all samples, while the potential electrodes for the 4-electrode resistivity and the S-wave transducers failed in some cases.

3.3.1 Measurements on sample K51:

The measurement records of sample K51 are shown in Fig. 4. The 4-electrode resistivity values turned out to be unreliable because point electrodes with insufficient contact

to the sample were used for the potential measurement. This 4-electrode coupling effect is present in the EIS measurements as well. Nevertheless, EIS-measurements are frequency-selective and thus hardly affected by noise. A mechanical defect occurred at 85 °C and oil from the confining pressure system intruded the sample.

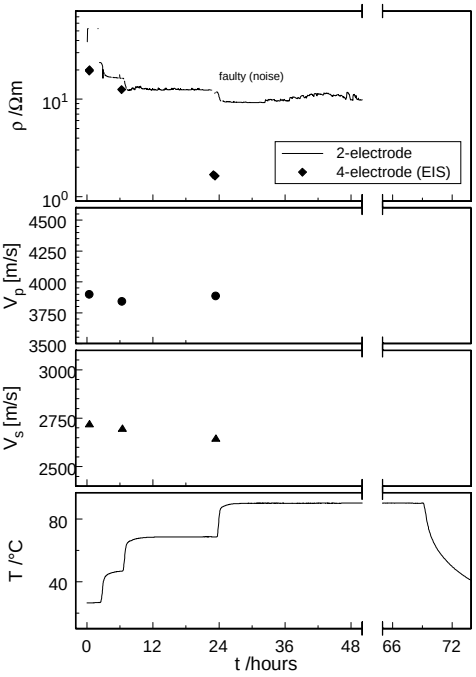

Figure 4: Measuring record, sample K51. The results of the resistivity monitoring are faulty. The EIS measurements are more trustworthy, because they are not affected by noise.

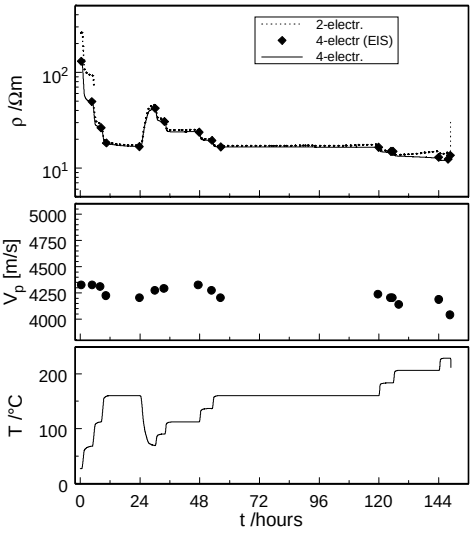

Figure 5: Measuring record, sample K52. The results of the resistivity monitoring are faulty. The EIS measurements are more trustworthy, because they are not affected by noise.

3.3.2 Measurements on sample K52:

The results from sample K52 are shown in Fig. 5. The 4-electrode resistivity with point electrodes were still used and the values are not trustworthy for the same reason as for K51. The pore pressure had to be raised at 120 °C to prevent the pore fluid from boiling, but this increase resulted in a leakage through the PTFE-jacket that terminated the experiment.

3.3.3 Measurements on sample K58

The experiment on sample K58 was split in two parts and the sample was run through 4 heating cycles, the final one up to 230 °C. The records are shown in Figs. 6 and 7. The 4-electrode resistivity setup was enhanced for the second cycle, yielding trustworthy results, although the cable isolations failed during the experiment, probably at the highest temperature.

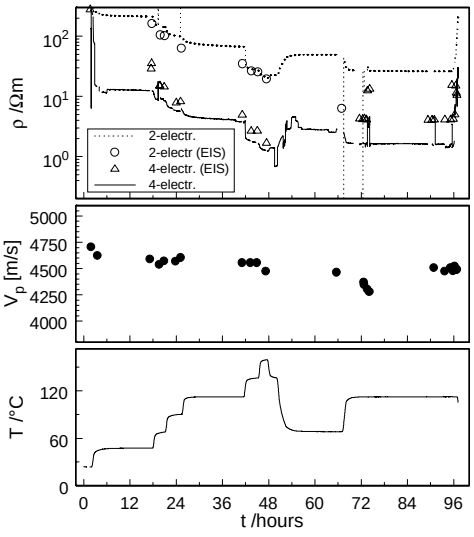

Figure 6: Measuring record sample K58, first experiment. Two heating cycles. The contact of the potential electrodes was improved, now both types of resistivity measurements are fairly according and trustworthy.

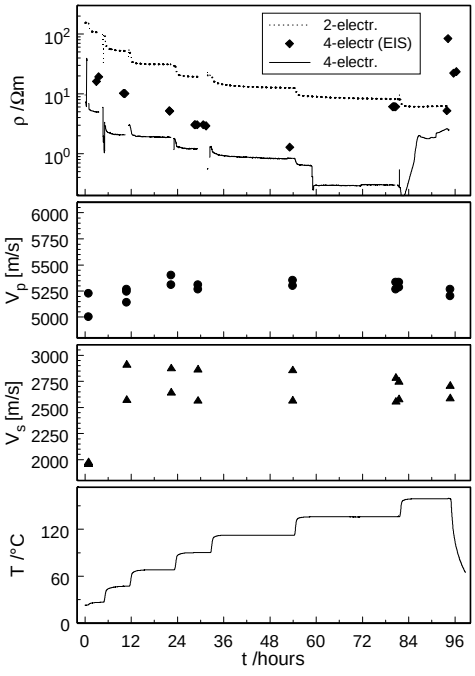

Figure 7: Measuring record, sample K58, second experiment, two heating cycles.

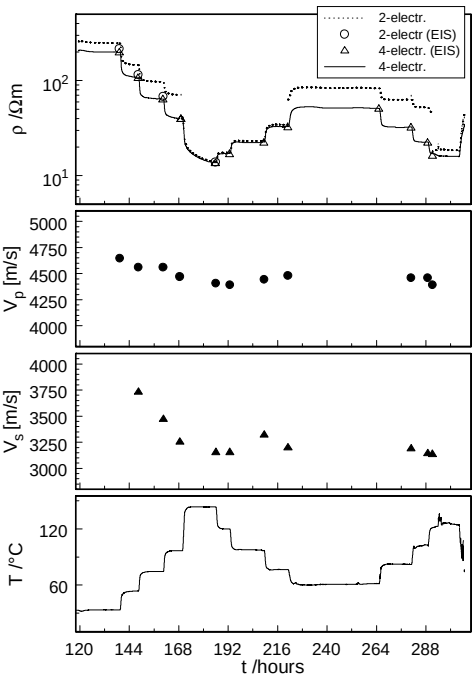

Figure 8: Measuring record, sample K9, first experiment, two heating cycles.

3.3.4 Measurements on sample K9

This experiment on sample K9 was split in two parts with 3 heating periods. The records are shown in Figs. 8 and 9. In the second part the S-wave transducers were defective, therefore only the P-wave velocities were recorded.

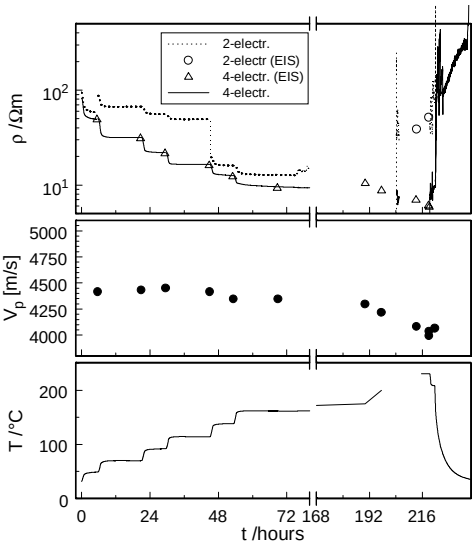

Figure 9: Measuring record, sample K9, second experiment.

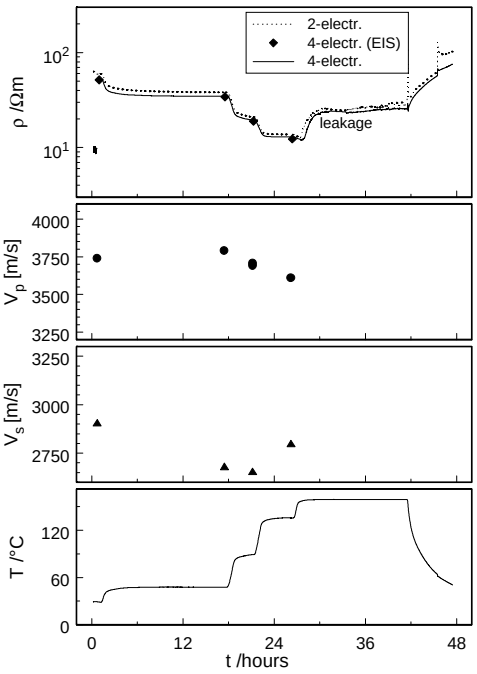

Figure 10: Measuring record, sample NJ6.

3.3.5 Measurements on sample NJ6

The experiment with sample NJ6 (Fig. 10) failed at a temperature of 150 °C. The S-wave transducers were defective, therefore only the P-wave velocities were recorded. At 150 °C a leakage through the jacket occurred and the sample was intruded by oil.

3.3.6 Measurements on sample NJ1

This experiment was successfully run through 2 heating cycles up to 230 °C (Fig. 11). Sudden oil leakage at oven temperature of 250°C cause oil leakage and terminated the experiment.

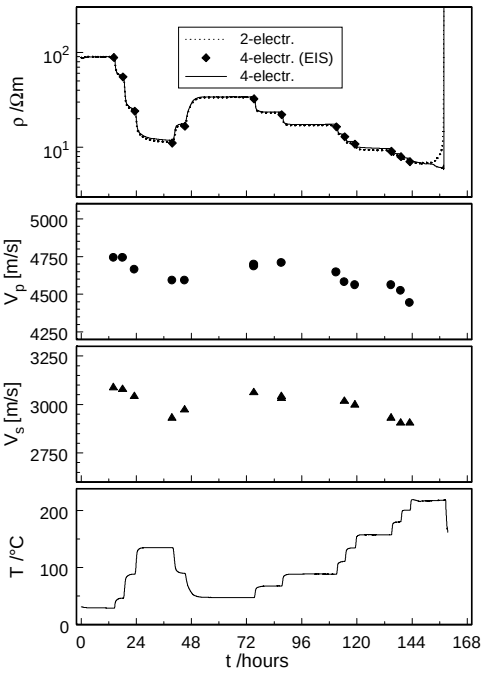

Figure 11: Measuring record, sample NJ1. Two heating cycles.

3.4 Experimental results

The presentation of conductivity versus temperature is superior to resistivity since the conductivity depends linearly on temperature. The conductivity showed generally a sudden change during the first heating cycle at temperature below 150 °C, but after that the repeatability was excellent. This behavior is shown in Figs. 12-14. It could be caused by dissolution of salts that precipitated in the pore space or by re-opening of micro-fractures that possibly have been closed during the drying and the long storage period.

The sample K58 (Fig. 14) showed a similar decrease in the compressional velocity at the same time with the conductivity jump. Therefore an effect of thermal cracking could be suspected. However, both P- and S-wave velocities of K9 (Fig. 13) and Nj1 (Fig. 12) apparently respond continually and repeatable to the temperature already at the first heating cycle. If newly formed micro-cracks were the cause for the conductivity jump they would most likely affect strongly the mechanical properties.

3.4.1 Temperature Dependence of Conductivity

The constant-phase-angle frequency dependence in the frequency range from 0.01 Hz to 1 kHz, which is accompanied by a conductivity increase with frequency, is not considered here. Mean values of the conductivity over the frequency range from 1 Hz to 1 kHz were calculated instead.

It has to be considered that the empirical approximation Eq. (1) is valid only for a limited temperature range near the reference temperature. Otherwise extrapolation to lower temperatures could yield false, even negative, conductivity values. However, the temperature dependence of the samples K9, K58 and NJ1 (Figs. 12-14) appears to follow a linear law up to 230 °C.

Temperature coefficients α calculated according to Eq. (1) from these data for a reference temperature of 20 °C are generally much higher than the assumed value for free water, 0.02 /°C. At the same time extrapolation to the reference conductivity σ_0 at 20 °C yields negative values, which is an indication for the limited range of validity of the linear equation.

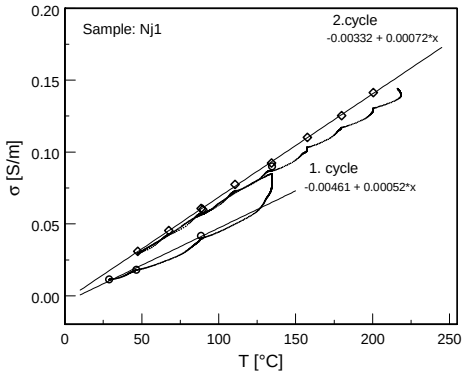

Figure 12: Temperature dependence of the electrical conductivity, Sample NJ1.

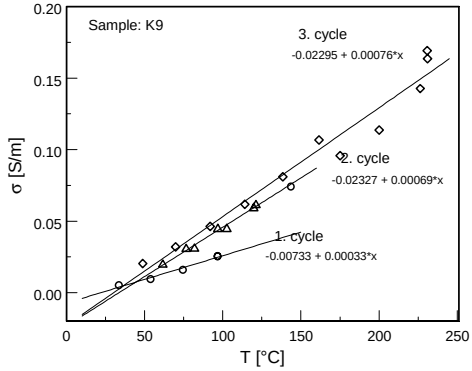

Figure 13: Temperature dependence of the electrical conductivity for three heating cycles, Sample K9.

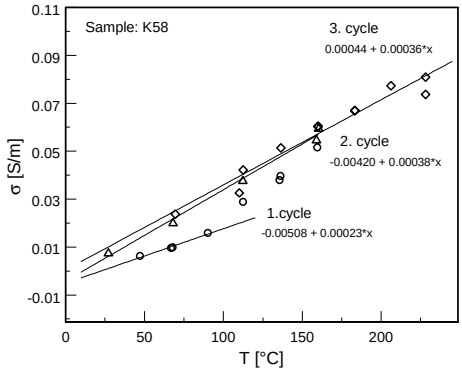

Figure 14: Temperature dependence of the electrical conductivity, Sample K58.

Fig. 15 shows the results from the second and third heating circles for the three sucessful samples compared to curves calculated from Eq (1) for different value of the temperature coefficient, α. In all the cases the temperature dependence of the samples are much higher than would be expected from pore fluid conduction (α =0,02). The sample K-58, from the smectite alteration zone, show roughly linear relationship with α in the range 0,04-0,05. This is similar to earlier reported values for samples where surface conducion in dominating (Flovenz et al 1985, Revil et al 1996). The two samples from the chlorite zone show still stronger temperature dependence. The dependence for the sample NJ1 is quite linear of the whole measeured temperature range with α = 0.065. The other sample, K9, shows large deviations from linear relationship, especially at temperatures above 150°C.

Our results for these three samples indicate that surface conduction is the dominant conduction mechanism for the samples, both from the smectite and the chlorite alteration zones at reservoir conditions, provided that the observed reverisible temperature effects on the conductivity is not caused by some reverisble chemical or mechanical processes in the samples during heating and cooling. This indication is supported by the result of measurements of the conductivity of similar samples as function of pore fluid conductivity (Flóvenz et al. 2005).

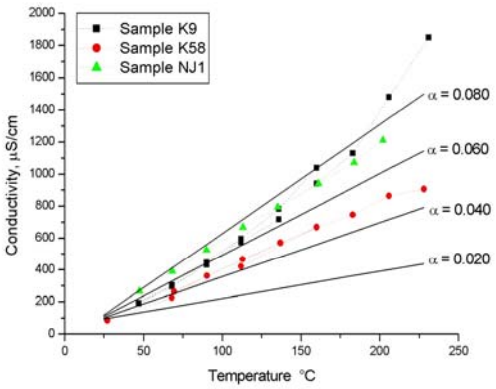

Figure 15: Temperature dependence of the conductivity of the three successful experiments. Data from second and third heating circles are included. The solid lines are theoretical lines calculated according to Eq. (1) with reference temperature 20°C and σ_0=85 µS/cm. Samples K9 and NJ1 that are from the chlorite alteration zone are much more temperature dependent than the sample K58 from the smectite alteration zone, both indicating high degree of surface (interface) conduction.

3.3.2 Temperature Dependence of Ultrasonic P-and S-Wave Velocities

Both P- and S-wave velocities appear strongly and continually to decrease with temperature (Fig. 16-18). This effect is due to the behavior of the pore water, although the porosity is low.

The Wyllie-equation (time-average)

$$V_{P0}(T) = \left[\frac{\Phi}{V_{PW}(T)} + \frac{1-\Phi}{V_{Pmtx}} \right]^{-1} \qquad (4)$$

is suited as a simple model for the temperature dependence of ultrasonic P-wave velocity, where Φ, V_{P0}, V_{PW}, V_{Pmtx} are porosity, sound velocity in the fluid saturated rock, in the water, and in the solid material, respectively. The temperature dependence of water is known (Fig. 2). The results from Eq. (4) are in good agreement with the measuring results. It appears that the temperature dependence of the P-wave velocity reflects the temperature dependence of the sound velocity in the fluid.

Dissolution of salts and reopening of micro fractures would result in a decrease of the ultrasonic velocities. This decrease would affect the matrix velocity (V_{mtx}) and probably masks the increase predicted by Eq. (4) and the sound speed of the fluid (Fig. 2) in the low temperature range up to 100 °C.

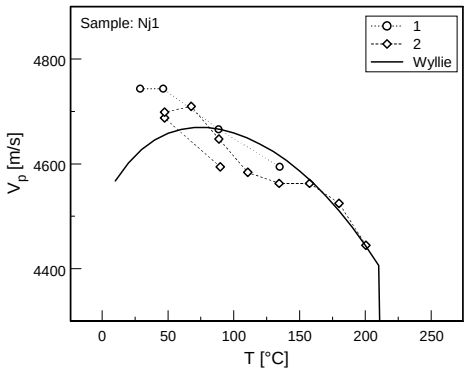

Figure 16: Temperature dependence of the compressional velocity for two heating cycles. The model line is calculated with Φ=10%, V_{Pmtx}=6000 m/s.

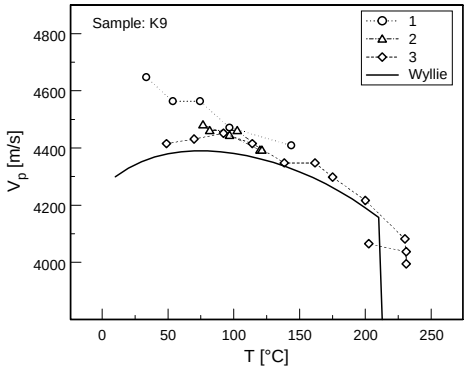

Figure 17: Temperature dependence of the compressional velocity. The model line is calculated with Φ=10%, V_{Pmtx}=5500 m/s.

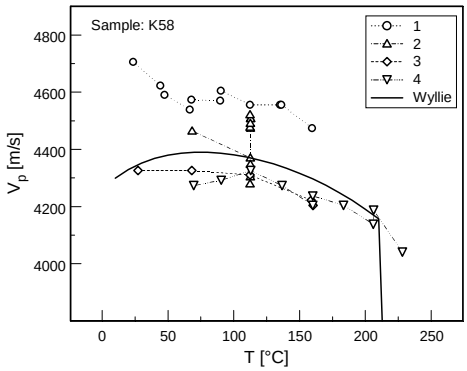

Figure 18: Temperature dependence of the compressional velocity. The model line is calculated with Φ=10%, V_{Pmtx}=5500 m/s.

The temperature dependence of the shear velocity should be related more to the properties of the solid framework. This explains its only slight temperature dependence (Figs. 19 and 20), compared to the P-wave velocity, at temperatures above 100 °C.

Because of its sensitivity to changes in the solid framework it should reflect low temperature alterations like fracturing or dissolution of cements to a higher degree. However, the experimental data basis does not allow general conclusions with respect to the shear wave velocity yet.

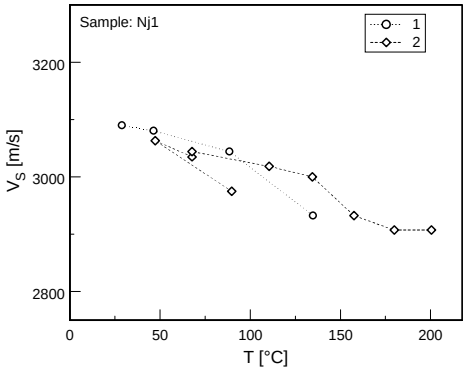

Figure 19: Temperature dependence of the shear wave velocity, sample NJ1.

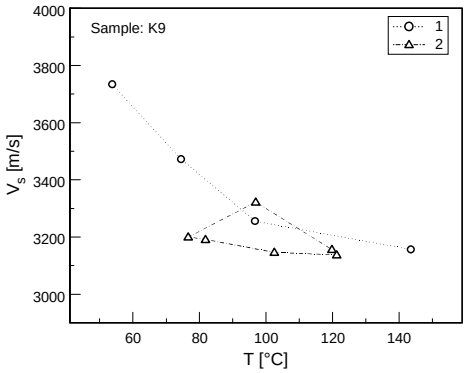

Figure 20: Temperature dependence of the shear wave velocity, sample K9.

4. CONCLUSIONS

Three out of six samples were exposed to temperatures up to 250 °C at the due pore pressure to keep the pore water liquid for periods up to some days. The material was basaltic volcanic rock, saturated with low saline water.

In spite of the rather complicated physical causes for electrical conduction in rocks, which probably influence the elastic properties as well, simple linear temperature dependences could be found for the conductivity. However, the temperature coefficients are very high in most cases, probably reflecting the influences of fluid-solid interaction (surface conductivity) or from alteration effects, which are possibly reversible. The high temperature dependence is both observed for samples from the smectite and the chlorite zone. This contradicts the hypothesis of Arnason and Flovenz (1992) that the increased resistivity in the chlorite zone of geothermal fields is due to change from surface conduction in the smectite zone to pore fluid conduction in the chlorite zone.

The temperature dependence of the compressional velocity is controlled by the fluid effect. The strong temperature dependence of the sound speed of water causes corresponding strong decrease of the compressional velocity of the rock at temperatures above 100 °C. The simple time-average equation in combination with the sound speed of pure water is a suitable model for its temperature dependence. A stronger decrease of both compressional and shear wave velocity at temperatures below 100 °C that contradicts the fluid behavior may be due to reopening of micro-cracks or dissolution of precipitated salts.

There is still need for research, mainly for similar laboratory measurements like this study, because the data basis for the evaluation of high-temperature reservoirs is weak. Some standard methods, which are generally used, like the Arps-formula for the electrical conductivity of brines, become wrong at temperatures exceeding 150 °C. The results from this study show that fluid-rock interactions considerably influence the temperature dependence of physical rock properties.

REFERENCES

Arnason, K., and Flóvenz, O.G.: Evaluation of physical methods in geothermal exploration of rifted volcanic crust. GRC Transactions, vol. 16, 207-217, 1992

Arnasson, K., Karlsdottir, R., Eysteinsson, H., Flovenz, O.G., and Gudlaugsson, S.T.: The Resistivity Structure of High-Temperature Geothermal Systems in Iceland, Proceedings, World Geothermal Congress, Kyushu-Tohoku (2000)

Arps, J.J.: The effect of temperature on the density and electrical resistivity of sodium chloride solutions. Petr. Trans. AIME, 198, 327-330.

Duba, A., Roberts,J., and Bonner,B. (1997): Electrical properties of geothermal reservoir rocks as indicators of porosity distribution. Proceedings, 22th Workshop on Geothermal Reservoir Engineering Stanford University, Stanford, California, January 27-29, 1997

Fernandez, D.P., Goodwin, A.R.H., Lemmon, E.W., Levelt Sengers, J.M.H., and Williams, R.C.: A Formulation for the Static Permittivity of Water and Steam at Temperatures from 238 K to 873 K at Pressures up to 1200 MPa, Including Derivatives and Debye-Hückel Ceofficients. J. Phys. Chem. Ref. Data, 26, 4, 1125-1162, 1997

Flóvenz, Ó.G., Georgsson, L.S., and Árnason, K.: Resistivity Structure of the Upper Crust in Iceland, *J. Geophys. Res.*, 90, 10136-10150, 1985.

Flóvenz, Ó.G., Spangenberg, E., Kulenkapff, J., Árnason, K., Karlsdottir, R., and Huenges, E.: The role of interface conduction in geothermal exploration. Proceedings of the World Geothermal Congress, Antalya, turkey, 24-29 April 2005.

Franck, E.U., and Weingärtner, H.: Supercritical Water, in "Chemical Thermodynamics" (ed. Letcher, T.), IUPAC monography, Blackwell Science, 1999.

Ho, C.P., Palmer, D.A., Mesmer, R.E. : Electrical conductivity Measurements of Aqueous Sodium Chloride Solutions to 600°C and 300 MPa. J. Solution Chemistry, Vol. 23, 9, 997-1018, 1994.

Israelachvili, J.: Intermolecular and Surface Forces. Academic Press, London, 1992.

Kulenkampff, J., and Spangenberg, E.: Physical properties of cores from the Mallik 5L-38 production research well under simulated in situ conditions using the Field Laboratory Experimental Core Analysis System (FLECAS). In: Scientific Results from Mallik 2000 Gas Hydrate Production Research Well Program, Mackenzie Delta, Northwest Territories, Canada, (ed.) S.R. Dallimore and T.S. Collett; Geological Survey of Canada, Bulletin

Lemmon, E.W., McLinden, M.O., and Friend, D.G.: "Thermophysical Properties of Fluid Systems" in NIST Chemistry WebBook, NIST Standard Reference Database Number 69, Eds. P.J. Linstrom and W.G. Mallard, March 2003, National Institute of Standards and Technology, Gaithersburg MD, 20899 (http://webbook.nist.gov)

Llera, F.J., M. Sato, K. Nakatsuka, and Yokoyama, H.: Temperature dependence of the electrical resistivity of water-saturated rocks, Geophysics, 55, 576-585, 1990.

Reppert, P. M., and Morgan, F.D.: Temperature-dependent streaming potentials: 1. Theory. J. Geoph. Research, vol. 108, B11, 2546.

Revil, A., Cathles III, L. M., Losh, S., and Nunn, J. A.: Electrical Conductivity in Shaly Sands with Geophysical Applications. J. Geoph. Research, vol. 103, B10, 23925-23936.

Rink, M., and Schopper, J.R.,: Interface conductivity and its implication to electric logging. In: SPWLA 15th Ann. Logg. Symp. Trans., pp. 1–15, 1974.

Ucok, H., Ershaghi, I., Olhoeft, G.R.: Electrical resistivity of Geothermal Brines. JPT, April 1980, 717-727.

Ussher, G., Harvey, C., Johnstone, R., and Anderson, E.: Understanding the Resistivities Observed in Geothermal Systems, Proceedings, World Geothermal Congress, Kyushu-Tohoku (2000)